



# Highly transparent plasticized PVC composite film with ideal ultraviolet/high-energy short-wavelength blue light shielding

Keshun Su<sup>1,2</sup>, Yiyi Tao<sup>1,2</sup>, and Jun Zhang<sup>1,2,\*</sup>

<sup>1</sup>Department of Polymer Science and Engineering, College of Materials Science and Engineering, Nanjing Tech University, Nanjing 211816, China

<sup>2</sup>Jiangsu Collaborative Innovation Center for Advanced Inorganic Function Composites, Nanjing 211816, China

Received: 20 May 2021

Accepted: 31 July 2021

Published online:

9 August 2021

© The Author(s), under exclusive licence to Springer Science+Business Media, LLC, part of Springer Nature 2021

## ABSTRACT

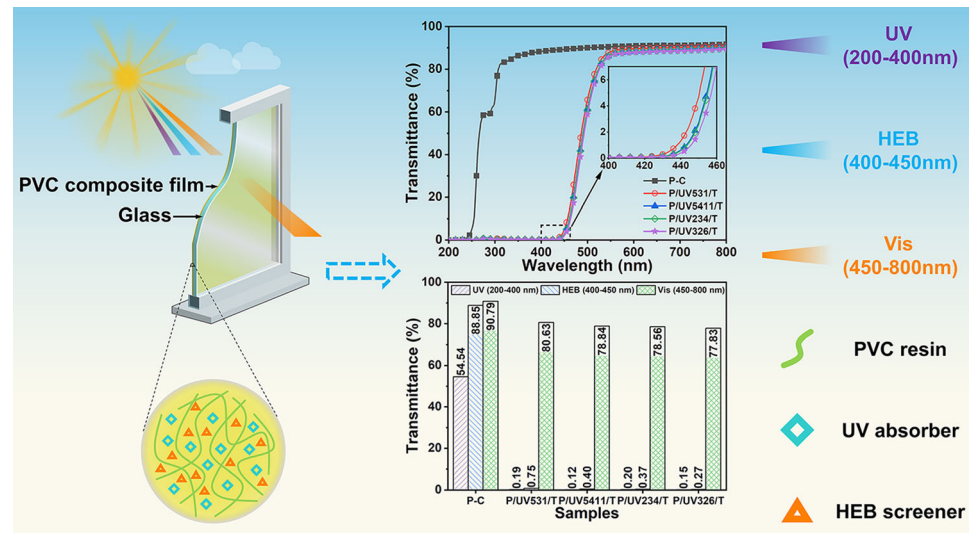
It is well known that ultraviolet light (UV) radiation is harmful to human health and affects the long-term stability of many organic materials. Besides, high-energy short-wavelength blue light (HEB) in the 400–450 nm range can penetrate the lens directly to the retina, causing visual damage. Therefore, these harmful solar radiations are pushing toward developing more efficient UV and HEB shielding materials. In this work, a design concept of highly transparent film with ideal UV/HEB shielding was brought forward. To achieve this concept, the UV absorbers and transparent yellow pigments with HEB filtering effect were selected as functional additives and introduced into plasticized polyvinyl chloride (PVC) by melt blending to improve the UV/HEB shielding performance of PVC. Firstly, we demonstrated that benzotriazole UV absorber UV326 has the optimal UV shielding rate (98%) compared to other types of UV absorbers and further confirmed that the HEB filtering of more than 99% could be achieved by adding 0.5 phr transparent yellow pigments. Moreover, the combination of UV absorbers and transparent yellow pigments makes all samples show more than 99% shielding effect in UV and HEB regions. At the same time, the stable mechanical properties of plasticized PVC composite film make it have great application value in the fields of building windows, automobile glasses, electronic screen films, spectacle lenses and LED lampshades.

Handling Editor: Maude Jimenez.

Address correspondence to E-mail: zhangjun@njtech.edu.cn

<https://doi.org/10.1007/s10853-021-06408-w>

## GRAPHICAL ABSTRACT



## Introduction

As is well known, ultraviolet light (UV) radiation of 200–400 nm is double-edged [1]. On the one hand, the short-wavelength UV (UVC, 200–280 nm) has the shortest wavelength, which leads to its maximum energy, so it has the effect of disinfection and sterilization [2]. Besides, medium-wavelength UV (UVB, 280–315 nm) also has beneficial effects such as promoting mineral metabolism and the formation of vitamin D in the body [3]. On the other hand, the long-wavelength UV (UVA, 315–400 nm) possesses strong penetrating power and can directly reach the dermis of the skin, destroying elastic fibers and collagen fibers, which can lead to skin tanning and an important cause of skin cancer [4]. Moreover, UV radiation not only has an important impact on people's health but also causes the photodegradation of organic matter such as polymers and colorants [5]. Blue light refers to the light of 400–500 nm in the visible light (Vis) region. According to the different wavelength ranges, it can be divided into high-energy short-wavelength blue light (HEB, 400–450 nm) and long-wavelength blue light (450–500 nm). HEB has extremely high energy, which can directly penetrate the lens to the retina, resulting in visual damage

[6]. However, long-wavelength blue light can regulate biological rhythm, and sleep, mood and memory are all related to it, which is beneficial to the human body [7]. Therefore, the daily blue light that damages our eyes mainly refers to HEB of 400–450 nm [8]. In addition to blue light emitted by natural light, computers, mobile phones, LED lights and other electronic products can also radiate different doses of HEB [9]. Thus, the development of new UV and HEB shielding materials has been received much attention.

In the past few years, people gradually realized the importance of developing UV shielding materials due to the harmful effects of UV radiation. Therefore, various materials have been used to prevent UV damage. Among them, common UV absorbers used in polymers are mainly divided into two types: inorganic oxides and organic compounds [10, 11]. Inorganic oxides such as titanium dioxide ( $\text{TiO}_2$ ) and zinc oxide (ZnO) have a wide band gap, and their absorption limit is just within the range of UV, so they can be used for UV shielding [12, 13]. Thien Vuong Nguyen et al. [14] prepared the high UV shielding nanocomposite coatings based on pure acrylic emulsion and R- $\text{TiO}_2$  or ZnO nanoparticles, and these coatings could shield more than 98% (for R- $\text{TiO}_2$ ) and 85% (for ZnO) of UV radiations. However, the photocatalytic performance and dispersion

degree of TiO<sub>2</sub> and ZnO seriously hinder their application [15, 16]. Organic UV absorbers mainly include salicylate, benzophenone and benzotriazole [17]. Salicylate is one of the UV absorbers that were earliest used by humans. Under the radiation of UV, it can form a benzophenone structure with strong UV absorbing ability through molecular rearrangement, thereby further enhancing its UV absorption ability [18]. However, its UV absorption range is narrow (< 340 nm), and the dihydroxy benzophenone and its derivatives generated after molecular rearrangement can absorb part of the Vis and appear yellow, which easily causes the material added with this UV absorber to turn yellow [2]. Benzophenone and benzotriazole UV absorbers are currently the most widely used UV absorbers [19]. Compared with the above-mentioned UV absorbers, they have the advantages of good compatibility with polymers, wide absorption range and excellent transparency. They can strongly absorb high-energy UV and exchange energy to consume or release energy in the form of heat or low radiation such as fluorescence and phosphorescence [20, 21].

Nowadays, inorganic nanoparticles whose absorbing edges are in the blue light region are generally added to the polymer matrix to achieve the purpose of shielding blue light. Commonly used inorganic nanoparticles include ZnO and cerium oxide (CeO<sub>2</sub>) [22]. Since the absorption edge of ZnO is in the UV region, it cannot be used alone to effectively block blue light. Therefore, the effective absorption of blue light is usually achieved by adding narrow band gap nanoparticles such as cadmium sulfide (CdS) and cadmium oxide (CdO) to red-shift the absorption edge of ZnO nanoparticles [23]. Chunchun Han et al. [24] prepared the epoxy-ZnO/CdS nanocomposites that can simultaneously shield UV and blue light and block more than 80% of blue light of 400–450 nm. Yanan Yang et al. [25] developed the ZnO/CdO thin films with high-energy blue light shielding function, and the average transmittance of the blue light between 400 and 450 nm is 54.55%. However, the toxicity of cadmium seriously hinders their wide application. For CeO<sub>2</sub> nanoparticles, due to their relatively small band gap, the absorption edge is just in the blue light region, so it can block blue light [26]. Yu Zhao et al. [27] synthesized the CeO<sub>2</sub> coated silicate microspheres core-shell particles to enhance the blue-light shielding property of polycarbonate composites. However, the addition of inorganic

nanoparticles also makes it lose the transmittance of Vis while achieving superior blue light blocking. In addition, the use of two materials with different refractive indexes to make a multilayer film can also effectively reduce the transmittance of blue light. Hsu et al. [28] prepared multilayer organic silicon and inorganic silicon oxide thin films on flexible polymer substrates using a high density inductively coupled plasma chemical deposition system. The results show that the stacked pair of 6 is favored, and it has a blue light transmittance of 58.4%. However, this method of preparing thin films is expensive and requires high precision in the thickness of the thin film. Apart from that, there are few reports on the use of organic yellow pigments as the blue light screeners. According to the complementary color principle, the complementary color corresponding to blue is yellow, so yellow pigments have the ability to absorb blue light [29]. Moreover, organic yellow pigments have the advantages of non-toxicity and low price.

In the study, the transparent plasticized PVC composite films with ideal UV/HEB shielding effects were prepared by adding UV absorbers and transparent yellow pigments to plasticized PVC resin. The effects of different types of UV absorbers on the UV shielding effect of plasticized PVC composite films were studied. Moreover, different amount of transparent yellow pigments was incorporated into the polymer matrix to investigate the optimal content. Finally, UV absorbers and transparent yellow pigments were added to the polymer matrix at the same time, and their synergistic shielding effect of UV and HEB was investigated.

## Design concept

A design concept that can achieve ideal UV/HEB shielding in the 200–800 nm region is shown in Fig. 1. It can be seen from Fig. 1a that when a piece of traditional glass without shielding ability attached to the window is irradiated by sunlight. The sunlight of 200–800 nm is perfectly irradiated into the room through the window, thus causing the UV and HEB transmitted through the window to affect the health of people and the long-term stability of organic matter. Therefore, the plasticized PVC composite film that can achieve ideal UV/HEB shielding in the range of 200–800 nm is proposed. As shown in Fig. 1b, when the pure plasticized PVC film is attached to the

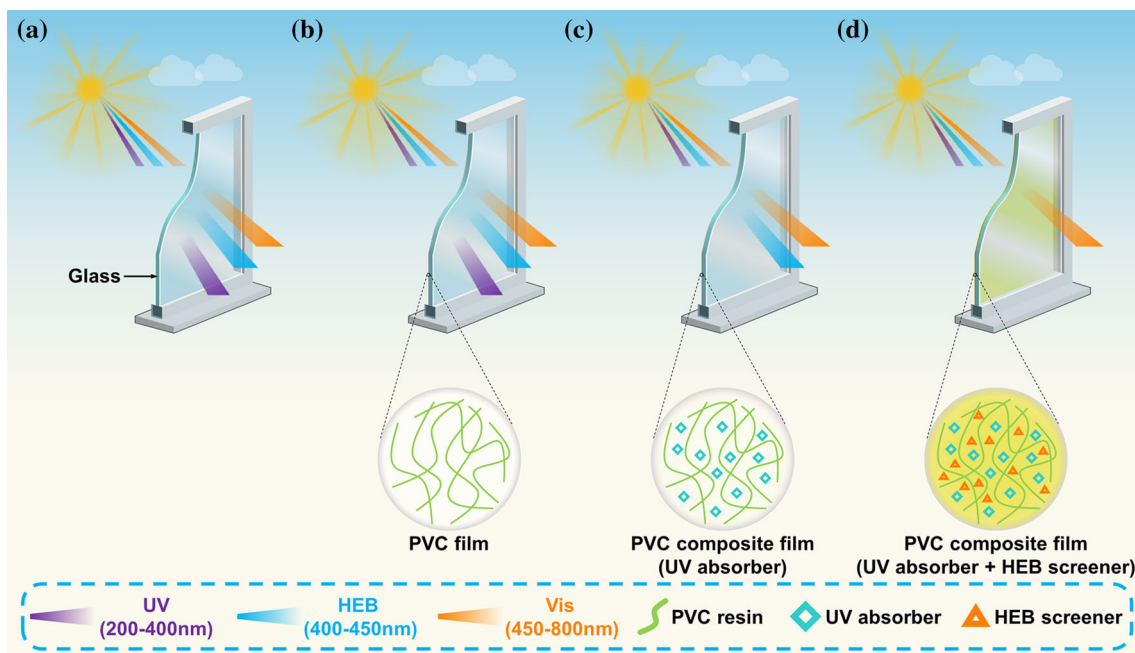


**Figure 1** The design concept of the plasticized PVC composite film: **a** Traditional glass; **b** PVC film is attached to the outside of the glass; **c** PVC composite film containing UV absorber is

attached to the outside of the glass; **d** PVC composite film containing UV absorber and HEB screener is attached to the outside of the glass. glass, the same result as Fig. 1a is presented due to the plasticized PVC film does not have a significant shielding effect on UV and HEB. Figure 1c shows that when the film with UV absorbers is attached to the glass, almost all the UV is absorbed after solar radiation, thus greatly avoiding the harm of UV. Figure 1d exhibits that when the plasticized PVC composite film prepared by adding the UV absorbers and HEB screeners is attached to the glass and is irradiated by sunlight, the UV and HEB are perfectly filtered out, thereby achieving the ideal UV/HEB shielding effect in the 200–800 nm region. The design concept only displays one aspect of the film applied to the window glass. In addition, the film can also be used in automobile glasses, electronic screen films, spectacle lenses and LED lampshades and other fields, thereby greatly reducing the harm of UV and HEB.

## Experimental

### Materials

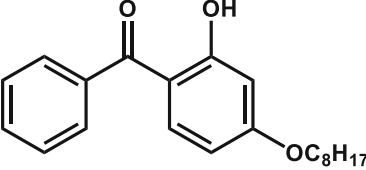
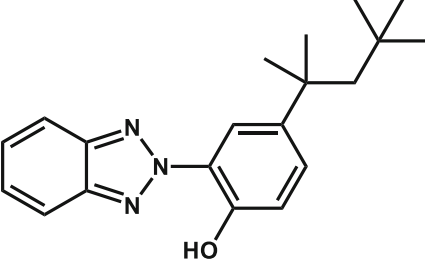
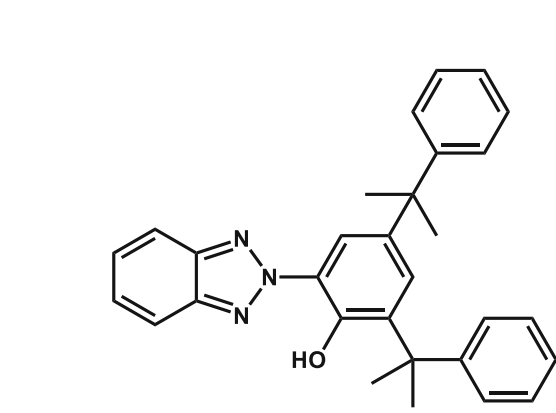
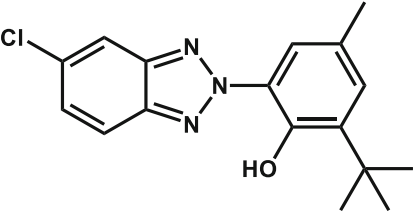
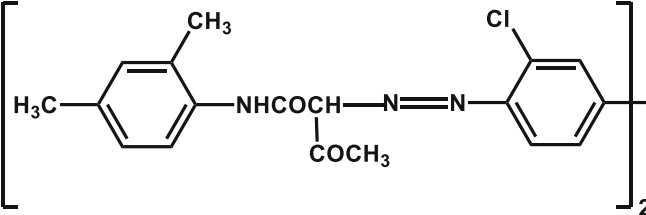
PVC resin (K67) was provided by Shanxi Yushe Chemical Co., Ltd., Jinzhong, China. Polyester plasticizer (PEP) was obtained from Zhangjiagang

Diasheng Chemical Co., Ltd., Zhangjiagang, China. Calcium stearate (CaSt) and zinc stearate (ZnSt) was supplied by Nanjing Jinling Chemical Plant Co., Ltd., Nanjing, China. Liquid paraffin and 1, 1, 2, 2-tetrachloroethane were purchased from Shanghai Lingfeng Chemical Reagent Co., Ltd., Shanghai, China. 2-(3-t-butyl-2-hydroxy-5-methylphenyl)-5-chlorobenzotriazole (UV326, CAS No. 3896-11-5) and 2-hydroxy-4-octyloxybenzophenone (UV531, CAS No. 1843-05-6) were produced by BASF Chemicals (China) Co., Ltd., Shanghai, China. 2-[3,5-bis(1-methyl-1-phenylethyl)-2-hydroxyphenyl] benzotriazole (UV234, CAS No. 70321-86-7) and 2-(2-hydroxy-5-tert-octylphenyl) benzotriazole (UV5411, CAS No. 3147-75-9) were provided by Nanjing Hualiming Co., Ltd., Nanjing, China. Transparent yellow pigment (Pigment Yellow 122, CAS No. 852620-87-2) was purchased from Nanjing Pinfu Industry and Trade Co., Ltd., Nanjing, China. The structures of these functional additives are shown in Table 1.

### Sample preparation

Firstly, the 100 phr PVC resin, 65 phr PEP, 0.8 phr CaSt, 0.2 phr ZnSt and 0.2 phr liquid paraffin were mixed in the electric blast drying oven at 120 °C for 20 min, in order to make PVC resin pre-plasticized to

**Table 1** The structures of different functional additives

Commercial name	Chemical structure
UV531	
UV5411	
UV234	
UV326	
Transparent yellow	

obtain pre-plasticized PVC. Then, the pre-plasticized PVC with the different proportions of UV absorbers and transparent yellow pigments were melted blending in a two-roll mill (SK 160B, Shanghai Rubber Machinery Works, Shanghai, China) at 160 °C to

obtain the sheet PVC compounds. The formulation of different proportions of pre-plasticized PVC and functional additives was shown in Table 2. After that, the film with regular thickness was prepared by hot molding on the plate vulcanizing press (XLB-D

**Table 2** Formulation of the plasticized PVC composite films added with different functional additives

Samples	Composition/phr					
	Pre-plasticized PVC	UV531	UV5411	UV234	UV326	Transparent yellow
P-C	166.2	–	–	–	–	–
P/UV531	166.2	0.5	–	–	–	–
P/UV5411	166.2	–	0.5	–	–	–
P/UV234	166.2	–	–	0.5	–	–
P/UV326	166.2	–	–	–	0.5	–
P/T-0.1	166.2	–	–	–	–	0.1
P/T-0.3	166.2	–	–	–	–	0.3
P/T-0.5	166.2	–	–	–	–	0.5
P/T-0.7	166.2	–	–	–	–	0.7
P/UV531/T	166.2	0.5	–	–	–	0.5
P/UV5411/T	166.2	–	0.5	–	–	0.5
P/UV234/T	166.2	–	–	0.5	–	0.5
P/UV326/T	166.2	–	–	–	0.5	0.5

phr = parts by weight per hundred parts of PVC resin

Pre-plasticized PVC contains 100 phr PVC resin, 65 phr PEP, 0.8 phr CaSt, 0.2 phr ZnSt and 0.2 phr liquid paraffin

350 × 350 × 2, Shanghai First Rubber Machinery Factory, Shanghai, China) at 160 °C. Finally, the film was further processed to obtain the standard sample for subsequent characterization tests.

## Characterizations

### Fourier transformed infrared spectroscopy (FTIR)

The infrared spectra of different functional additives and the plasticized PVC composite films with a thickness of  $30 \pm 5 \mu\text{m}$  were measured by transmission mode of FTIR spectrometer (Nicolet IS5, Thermo Fisher, USA). For all scans, the spectra were collected over the region ranging from 400 to  $4000 \text{ cm}^{-1}$ , with a resolution of  $4 \text{ cm}^{-1}$ .

### Digital photos

The digital photos of the plasticized PVC composite films with a diameter of 23 mm and a thickness of  $0.3 \pm 0.02 \text{ mm}$  were taken by a smartphone (iPhone xs, Apple Inc., USA).

### Ultraviolet–visible spectrophotometer (UV–Vis)

The absorbance of different functional additives and transmittance of the plasticized PVC composite films added with different functional additives were investigated by a UV–Vis spectrophotometer (UV-

3200, Shanghai Mapada Instruments Co., Ltd., Shanghai, China.). For the absorbance tests of different functional additives, UV531, UV5411, UV234, UV326 and transparent yellow pigments were dissolved in 1, 1, 2, 2-tetrachloroethane with moderate concentration ( $0.008 \text{ g/L}$ ), respectively. The air was used as a reference baseline, then the background of the 1, 1, 2, 2-tetrachloroethane solvent was excluded, and the sample was measured at room temperature in the region of 200–800 nm (200–400 nm for the UV region, 400–450 nm for the HEB region and 450–800 nm for the Vis region) with a scanning step of 1 nm. In addition, the molar absorption coefficient  $\varepsilon$  is calculated by the Lambert–Beer law, Eq. (1):

$$A = \log_{10} \left( \frac{P_0}{P} \right) = \varepsilon cl \quad (1)$$

where  $A$  is the absorbance;  $P_0$  and  $P$  are the intensity of incident monochromatic light and intensity of transmitted light, respectively;  $\varepsilon$  is the molar absorption coefficient ( $\text{L/mol/cm}$ );  $c$  is the sample concentration ( $\text{mol/L}$ );  $l$  is the optical path length ( $\text{cm}$ ).

For the transmittance of the plasticized PVC composite films added with different functional additives, the air was used as a reference baseline, and the measurements were done at room temperature in the region of 200–800 nm (200–400 nm for the UV region, 400–450 nm for the HEB region and 450–800 nm for

the Vis region) with a scanning step of 1 nm. Moreover, the average transmittance ( $T$ ) of different solar wavebands can be calculated by the following Eq. (2) [30]:

$$\bar{T} = \frac{\int_{\lambda_1}^{\lambda_2} T(\lambda)d\lambda}{\lambda_2 - \lambda_1} \tag{2}$$

where  $T$  is the average transmittance (%) of different solar wavebands;  $T(\lambda)$  is the transmittance value for a certain ( $\lambda$ );  $\lambda_1$  and  $\lambda_2$  are the minimum and maximum values of different solar wavebands, respectively.

*Mechanical properties*

The universal testing machine (CMT 5254, Shenzhen SANS Testing Machine Co., Ltd., Shenzhen, China) was applied for the measurement of tensile properties and tear properties of the samples at a testing rate of 50 mm/min. Three replicates were made for each sample, and the average values with standard deviation have been reported. Shore A durometer (LX-A, Jiangsu Mingzhu Testing Machinery Co., Ltd., Yangzhou, China) was used to measure the hardness of samples, according to ISO 7619–1:2004. For each sample, the hardness of resident time at 0 s and 15 s was measured 5 times, and the average value was taken as the hardness value of 0 s and 15 s, respectively. Before testing, all the samples were pretreated in standard testing conditions ( $23 \pm 2$  °C temperature and  $50 \pm 5\%$  relative humidity) for 12 h to prevent the temperature from affecting the mechanical properties of the plasticized PVC composite films.

**Results and discussion**

**Absorption mechanism**

The absorption spectra of different functional additives at the same mass concentration are shown in Fig. 2a. Figure 2b shows the molar absorption coefficient curves of different functional additives, reflecting the absorbance when the concentration of the light-absorbing substance is 1 mol/L and the thickness of the absorption cell is 1 cm. Compared with the absorption spectra, the molar absorption coefficient curves can more accurately compare the absorption ability of different light-absorbing substances at the same wavelength. For UV absorbers, as shown in the figure, the three benzotriazole UV absorbers UV5411, UV234 and UV326 have similar absorption peak shapes due to their similar structures. According to the data in Fig. 2 and Table 3, compared to the benzophenone UV531, the benzotriazole UV absorbers have a higher molar absorption coefficient, and both  $\lambda_{max1}$  and  $\lambda_{max2}$  have a red-shift, which makes them show a steeper absorption edge near the wavelength of 400 nm, indicating that benzotriazole UV absorbers have higher absorption efficiency, wider absorption range and better light stability than benzophenone UV absorbers. In addition, the hydrogen on the benzotriazole ring in UV326 is replaced by chlorine. As a result,  $\lambda_{max1}$  and  $\lambda_{max2}$  showed a red-shift and a slight increase in molar absorption coefficient compared with chlorine-free UV234 and UV5411, indicating that the energy between the ground state and excited state decreased, which made them more favorable for UV absorption, thus showing the excellent UV absorption range (200–402 nm). For transparent yellow pigments, combining with the data in Fig. 2 and Table 3, it can be seen that the two largest absorption peaks of

**Figure 2** a Absorption spectra of different functional additives; b Molar absorption coefficient curves of different functional additives.

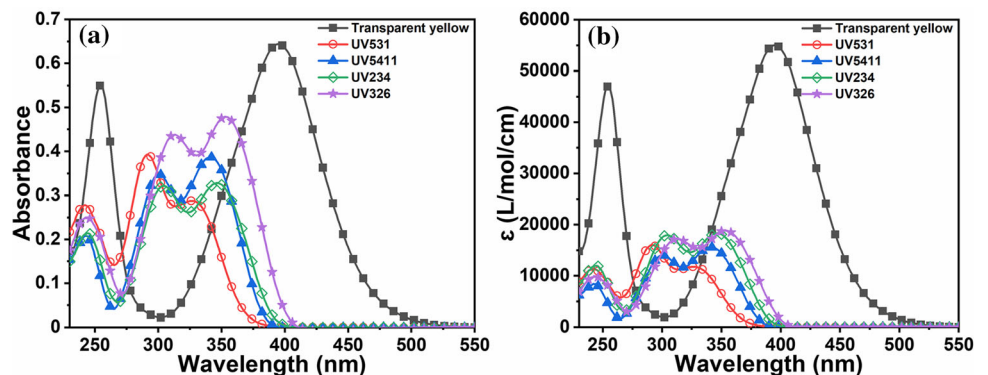
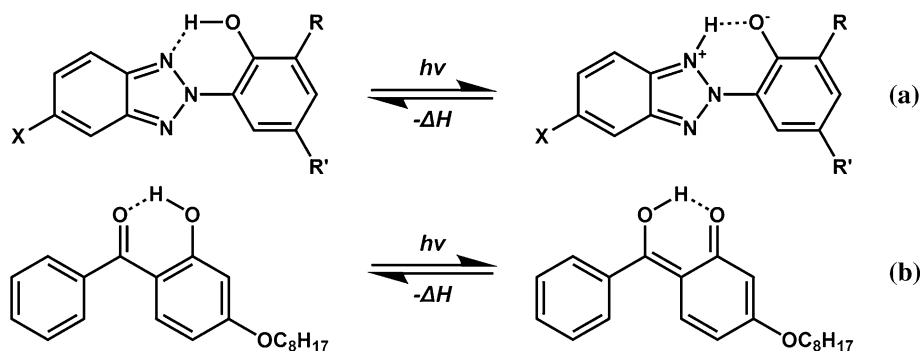


**Table 3** Absorption parameters of different functional additives

Commercial name	$\lambda_{\max_1}/(\text{nm})$	$\varepsilon_1/(\text{L/mol/cm})$	$\lambda_{\max_2}/(\text{nm})$	$\varepsilon_2/(\text{L/mol/cm})$	Absorption region/(nm)
UV531	326	11832	291	16421	200–371
UV5411	341	15656	301	14179	200–383
UV234	350	18319	304	18062	200–392
UV326	355	18853	313	17279	200–402
Transparent yellow	395	55204	252	49016	200–507

$\lambda_{\max_1}$  and  $\varepsilon_1$  are the first UV absorption maximum peak and its molar absorption coefficient, respectively;  $\lambda_{\max_2}$  and  $\varepsilon_2$  are the second UV absorption maximum peak and its molar absorption coefficient, respectively; The absorption region is based on the molar absorption coefficient greater than  $10^3$  L/mol/cm as the standard

**Figure 3** Absorption mechanism of different types of UV absorbers: **a** the excited state intramolecular proton transfer mechanism of benzotriazole UV absorbers; **b** absorption mechanism of benzophenone UV absorbers.



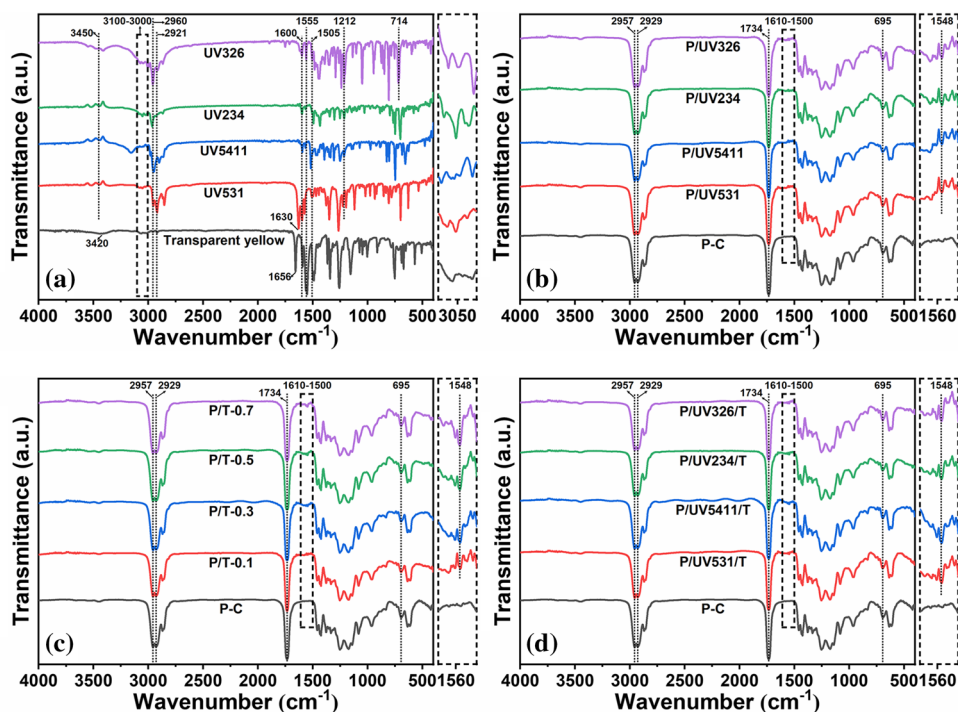
transparent yellow pigments are shown in the waveband range of 230–550 nm, indicating that the transparent yellow pigments possess strong absorption of short-wavelength UV at 200–280 nm and HEB at 400–450 nm. However, transparent yellow pigments have a weak absorption ability for UV around 300 nm, while UV absorbers have excellent absorption capability for UV in this wavelength range. Therefore, if the UV absorber is simply compounded with the transparent yellow pigment, it will be able to achieve perfect absorption of UV and HEB regions.

Figure 3a, b exhibit the UV absorption mechanism of benzotriazole and benzophenone UV absorbers, respectively. It can be seen from Fig. 3a that benzotriazole UV absorbers can strongly absorb high-energy UV and exchange energy to consume or release energy in the form of heat or low radiation such as fluorescence and phosphorescence [31]. Its mechanism of action is based on the conversion of absorbed light energy into heat energy by tautomer. Before absorbing light, UV absorbers exist in the form of phenolic compounds. Because the electron density on the oxygen atom is much greater than the electron density on the nitrogen atom of the triazole ring, it shows strong alkalinity. The absorption of light

makes the electrons density mainly shifts from the oxygen atom to the nitrogen atom of the triazole ring, which makes the phenol more acidic and the nitrogen atom more alkaline, and the proton quickly transfers to the nitrogen atom to form a tautomer [32, 33]. This tautomer is unstable and can safely convert excess energy into heat and return to a more stable ground state. The entire interconversion process is extremely efficient and can be repeated almost infinitely, which is the reason for its light stability. In addition, the introduction of halogen atoms or unsaturated bonds in the 5-position of benzotriazole can stabilize the alcohol structure, dilute the color of the product and increase the light transmittance [34]. Usually, the introduction of chlorine atoms can increase the molar absorption coefficient by 1.2 times and lead to a red-shift of the absorption wavelength. Therefore, UV326 is an excellent UV absorber. As shown in Fig. 3b, in the benzophenone structure, the hydroxyl hydrogen on the benzene ring and the adjacent carbonyl oxygen can form intramolecular hydrogen bonds to constitute a chelating ring [35]. After absorbing UV, the molecule undergoes thermal shock, and the hydrogen bond is broken, meanwhile, the chelating ring is opened [36]. At this time, the compound is in an



**Figure 4** FTIR spectra of different functional additives and all samples: **a** The different functional additives; **b** The plasticized PVC composite films added with different types of UV absorbers; **c** The plasticized PVC composite films added with different contents of transparent yellow pigments; **d** The plasticized PVC composite films added with UV absorbers and transparent yellow pigments.



unstable high-energy state, and excess energy is released in the process of returning to the original low-energy state, so the high-energy and harmful UV becomes low-energy and harmless heat energy [37]. In addition, when the carbonyl group is excited, tautomerism occurs to form the enol structure, which also consumes a part of energy [38].

### FTIR spectra

Figure 4 reports the infrared spectra of different functional additives and the plasticized PVC composite films added with different functional additives. The infrared spectra of UV absorbers and transparent yellow pigments are shown in Fig. 4a. For all functional additives, they have some same infrared peak positions, including multiple bands in the range of 3100–3000  $\text{cm}^{-1}$ , 2960  $\text{cm}^{-1}$ , 2921  $\text{cm}^{-1}$  and multiple bands near 1550  $\text{cm}^{-1}$ , which are attributed to the joint contribution of the aromatic ring C–H stretching vibration and the octave band of the aromatic ring skeleton vibration, the C–H stretching vibration on the methyl group, the C–H stretching vibration on the methylene group and the skeleton vibration of the benzene ring, respectively. The peaks around 3450  $\text{cm}^{-1}$  and 1212  $\text{cm}^{-1}$  correspond to the stretching vibration of the hydroxyl

group and the C–O bond on UV absorbers, respectively. In addition, the peaks at 1630  $\text{cm}^{-1}$  and 714  $\text{cm}^{-1}$  are caused by the C=O stretching vibration on UV531 and the C–Cl stretching vibration on UV326, respectively. For transparent yellow pigments, the vibration peaks around 3420  $\text{cm}^{-1}$  and 1656  $\text{cm}^{-1}$  are attributed to the stretching vibration of N–H and C=O, respectively. For the plasticized PVC composite films added with different functional additives, the peaks of 2957  $\text{cm}^{-1}$ , 2929  $\text{cm}^{-1}$ , 1734  $\text{cm}^{-1}$  and 695  $\text{cm}^{-1}$  mainly come from the contribution of the plasticized PVC film [39]. Several bands in the range of 1610–1500  $\text{cm}^{-1}$  were found in the plasticized PVC composite films added with different functional additives, mainly due to the skeleton vibration of the benzene ring on the functional additives, indicating that the functional additives have been successfully added into the plasticized PVC films. In addition, it can be seen from Fig. 4c that with the increase of the transparent yellow pigments content, the intensity of the peak around 1548  $\text{cm}^{-1}$  shows a gradually increasing trend. This result further shows that the transparent yellow pigments have been successfully added into the plasticized PVC films.

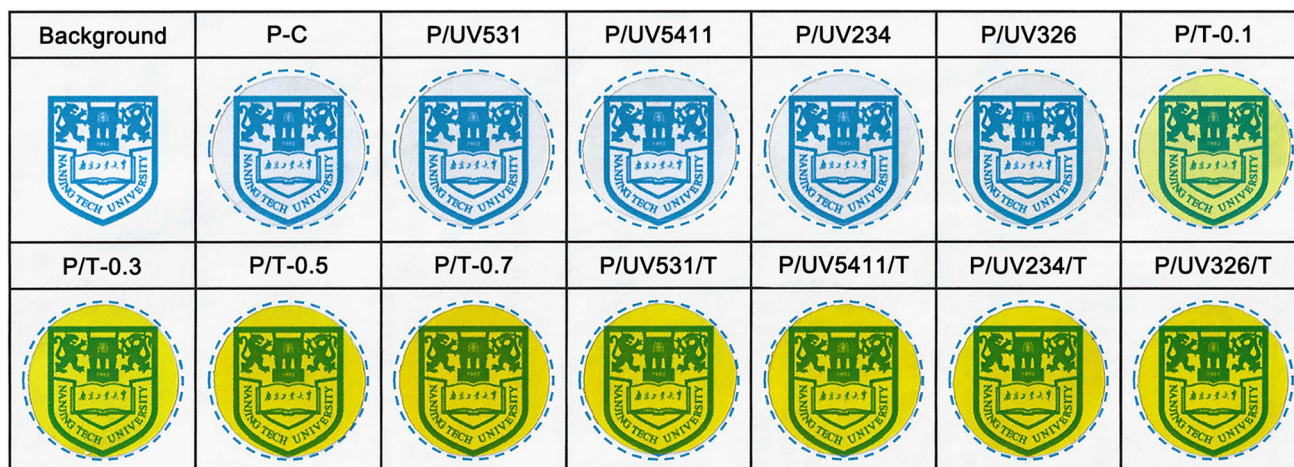


**Figure 5** Digital photos of the plasticized PVC composite films added with different functional additives.

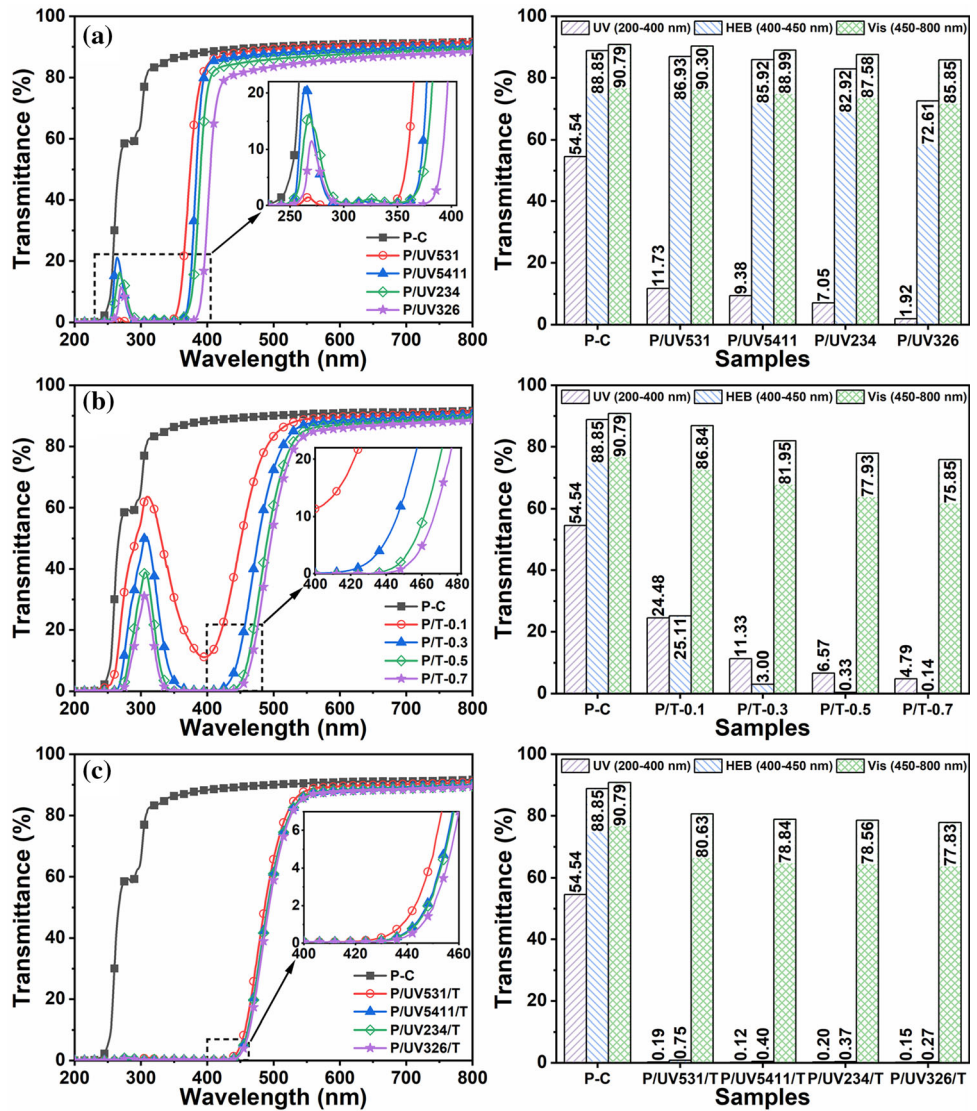
### Optical properties

Digital photos of the plasticized PVC composite films with different functional additives were taken to reveal the effects of different functional additives on the transparency of plasticized PVC composite films. Figure 5 shows the digital photos of all samples. It can be seen from the figure that the pure plasticized PVC film without added functional additives is colorless and transparent. When different UV absorbers are added, the PVC composite films still appear colorless and transparent, which is no different from pure plasticized PVC film to the naked eye, indicating that these UV absorbers only absorb UV, and do not significantly absorb Vis, thereby coloring the films. When transparent yellow pigments of different contents are added, all the samples appear yellow and transparent, and the yellow color of the PVC composite films gradually deepens with the increase of transparent yellow pigments content. When 0.5 phr UV absorbers and 0.5 phr transparent yellow pigments were added to PVC at the same time, all the samples showed a yellow color consistent with the 0.5 phr transparent yellow pigments added alone. In addition, the school badge at the bottom of the films is still clearly visible, reflecting that a small number of functional additives will not cause the transparency of the PVC composite films to show an intuitive change.

Figure 6 shows the transmittance spectra of plasticized PVC composite films with added different functional additives. It can be seen from Fig. 6a that when different types of UV absorbers are added, both

benzotriazole and benzophenone UV absorbers exhibit significant UV shielding effects. Among them, UV326 has the best UV shielding rate (98%). In contrast, the UV shielding rate of UV531 is relatively weak at 88%. This result is consistent with the result shown in Fig. 2 and once again shows that the UV shielding performance of benzotriazoles is better than that of benzophenones. In addition, compared to benzotriazole UV absorbers, UV531 has the least loss of Vis transmittance. This is because the absorption edge of UV326 is located at about 400 nm, which will cause some loss of Vis transmittance. Figure 6b shows the effect of adding transparent yellow pigments with different contents on the transmittance of each waveband of the plasticized PVC composite films. It can be seen from the figure that the HEB transmittance of all samples shows a significant decrease with the increase of transparent yellow pigments content. When the content of transparent yellow pigments is added to 0.5 phr, the HEB shielding rate of the plasticized PVC composite film has reached more than 99%. Therefore, under the condition that the Vis transmittance loss is small, the optimal addition amount of transparent yellow pigments is 0.5 phr. The effective absorption of transparent yellow pigments to the HEB is mainly attributed to the principle of complementary colors. In addition, the addition of 0.5 phr transparent yellow pigments makes the beneficial blue light of 450–500 nm still maintain the corresponding transmittance and will not significantly affect people's color perception and normal circadian rhythm. Figure 6c shows the transmittance spectra of the

**Figure 6** Transmittance curves and average transmittance of all samples: **a** The plasticized PVC composite films added with different types of UV absorbers; **b** The plasticized PVC composite films added with different contents of transparent yellow pigments; **c** The plasticized PVC composite films added with UV absorbers and transparent yellow pigments.



plasticized PVC composite films containing 0.5 phr UV absorbers and 0.5 phr transparent yellow pigments. It can be seen from the figure that the addition of the UV absorbers and the transparent yellow pigments simultaneously makes up for the shortcomings of the weak absorption of the single UV absorber for the 270 nm band and the strong transmission of the single transparent yellow pigments for the 300 nm band, making all films both show more than 99% UV/HEB shielding. In addition, UV531 obtained the best Vis transmittance (81%). This also shows that the combined use of UV absorbers and transparent yellow pigments can achieve ideal UV/HEB filtering. Due to the ideal UV/HEB shielding of the plasticized PVC composite film, it can be widely used in both indoor and outdoor environments, such as building

windows, automobile glasses, electronic screen films, spectacle lenses and LED lampshades. However, the ultimate applications will depend on their ability to resist deterioration of optical and mechanical properties after prolonged exposure. Therefore, artificial accelerated weathering experiments in the laboratory and natural weathering experiments will be further carried out in the future to observe the actual effect of weather resistance of plasticized PVC composite films with different combinations of UV absorbers and transparent yellow pigments.

### Mechanical properties

Mechanical properties are one of the most important properties that affect the application value of

**Table 4** Mechanical properties of the plasticized PVC composite films added with different functional additives

Samples	Tensile strength (MPa)	Elongation at break (%)	Modulus at 100% (MPa)	Tear strength (kN/m)	Shore A hardness (HA)	
					0 s	15 s
P-C	14.83 ± 0.34	350 ± 12	5.44 ± 0.23	46.10 ± 1.22	80 ± 0	71 ± 0
P/UV531	14.72 ± 0.48	358 ± 20	5.50 ± 0.11	45.44 ± 0.49	79 ± 0	70 ± 0
P/UV5411	14.84 ± 0.66	359 ± 17	5.27 ± 0.10	45.60 ± 1.26	78 ± 1	71 ± 0
P/UV234	15.19 ± 1.17	373 ± 21	5.53 ± 0.09	47.36 ± 1.60	77 ± 1	70 ± 1
P/UV326	15.06 ± 0.68	367 ± 7	5.48 ± 0.03	47.89 ± 2.38	77 ± 1	70 ± 1
P/T-0.1	15.73 ± 0.11	386 ± 13	5.23 ± 0.02	46.75 ± 1.77	77 ± 1	69 ± 1
P/T-0.3	15.01 ± 0.06	351 ± 8	5.52 ± 0.13	46.06 ± 0.99	79 ± 1	71 ± 2
P/T-0.5	15.27 ± 0.27	362 ± 8	5.40 ± 0.17	45.75 ± 0.65	79 ± 1	71 ± 0
P/T-0.7	15.65 ± 0.46	376 ± 22	5.45 ± 0.07	47.29 ± 1.10	78 ± 0	71 ± 1
P/UV531/T	15.31 ± 0.28	374 ± 15	5.13 ± 0.08	45.78 ± 0.27	79 ± 1	70 ± 1
P/UV5411/T	15.18 ± 0.74	375 ± 14	5.41 ± 0.08	46.60 ± 0.54	79 ± 1	70 ± 1
P/UV234/T	14.31 ± 0.11	346 ± 7	5.17 ± 0.05	45.28 ± 1.32	79 ± 1	71 ± 0
P/UV326/T	15.33 ± 0.25	377 ± 13	5.34 ± 0.12	45.59 ± 1.22	78 ± 1	70 ± 1

materials. The mechanical properties of plasticized PVC composites films added with different functional additives were measured to evaluate whether their mechanical properties were affected. The tensile properties, tear properties and Shore A hardness of all samples are shown in Table 4. For the tensile properties and tear properties, it can be seen from Table 4 that the tensile properties and tear properties of the plasticized PVC composite films did not change much with the addition of UV absorbers and transparent yellow pigments. The tensile strength, elongation at break, modulus at 100% and tear strength of all samples only have been slight oscillations in the ranges of 14–15 MPa, 350–370%, 5–6 MPa and 45–47 kN/m, respectively, indicating a small number of functional additives will not affect the movement of the PVC molecular chains and the rigidity of the material. The shore A hardness test can directly reflect the hardness of the material. The instantaneous hardness of all samples and the hardness after 15 s of contact between the pressure plate and the sample were tested. As shown in Table 4, compared with the pure plasticized PVC film without adding functional additives, the hardness change of the plasticized PVC composite films is negligible. For instantaneous hardness, the hardness value varies between 77 and 80°ShA. Similarly, the hardness of the pressure plate and the sample after contacting for 15 s vary between 69 and 71°ShA. This is because the

hardness of PVC material is closely related to the content of the plasticizer, and the content of the plasticizer in all samples is basically the same. In addition, a small number of functional additives will not affect the force between molecular chains, resulting in a significant change in hardness.

## Conclusions

In this study, a design concept of preparing a highly transparent film with ideal UV/HEB shielding was first proposed. We used benzotriazole and benzophenone as UV absorbers and transparent yellow pigments as HEB screeners, which were added to plasticized PVC substrate to prepare plasticized PVC composite films. Then the main research on the optical properties of plasticized PVC composite films is carried out. After different UV absorbers are added, the UV shielding performance of the plasticized PVC composite films is greatly improved. Among them, 98% UV shielding can be achieved by using UV326 as the UV absorber. When different contents of transparent yellow pigments are added, the HEB shielding rate of the plasticized PVC composite films increases significantly with the increase of transparent yellow pigments content. When the content of transparent yellow pigments is added to 0.5 phr, the HEB shielding rate has reached more than 99%. After mixing 0.5 phr UV absorbers and 0.5

phr transparent yellow pigments and adding plasticized PVC substrate, all samples have achieved more than 99% UV/HEB shielding. Among them, the plasticized PVC composites film with UV531 as the UV absorber has the highest Vis transmittance (81%). In addition, the stable mechanical properties of the plasticized PVC composite film make it have an extensive value in application. In summary, the results show that the plasticized PVC composite film has an ideal UV/HEB shielding effect, meanwhile, possesses an excellent transmittance in the Vis region. Therefore, it can be widely used in building windows, automotive glasses, screen films, spectacle lenses and LED lampshades.

The highly transparent plasticized PVC composite film with ideal UV/HEB shielding is introduced in this paper. In order to verify the effect of long-term use of the plasticized PVC composite film, artificial accelerated weathering experiments in the laboratory and natural weathering experiments will be carried out in the future to obtain more research results with practical application value.

## Acknowledgements

This work was supported by the Priority Academic Program Development of Jiangsu Higher Education Institution (PAPD).

## Declarations

**Conflict of interest** The authors declare that they have no known competing financial interests or personal relationships that could have appeared to influence the work reported in this paper.

## References

- [1] Hu D, Zhang Z, Liu M, Lin J, Chen X, Ma W (2020) Multifunctional UV-shielding nanocellulose films modified with halloysite nanotubes-zinc oxide nanohybrid. *Cellulose* 27:401–413. <https://doi.org/10.1007/s10570-019-02796-0>
- [2] Zhang Y, Naebe M (2021) Lignin: a review on structure, properties, and applications as a light-colored UV absorber. *ACS Sustain Chem Eng* 9:1427–1442. <https://doi.org/10.1021/acssuschemeng.0c06998>
- [3] Tu Y, Zhou L, Jin YZ, Gao C, Ye ZZ, Yang YF, Wang QL (2010) Transparent and flexible thin films of ZnO-poly-styrene nanocomposite for UV-shielding applications. *J Mater Chem* 20:1594–1599. <https://doi.org/10.1039/b914156a>
- [4] Mueen R, Morlando A, Qutaish H, Lerch M, Cheng Z, Konstantinov K (2020) ZnO/CeO<sub>2</sub> nanocomposite with low photocatalytic activity as efficient UV filters. *J Mater Sci* 55:6834–6847. <https://doi.org/10.1007/s10853-020-04493-x>
- [5] Zhao ZT, Mao AR, Gao WW, Bai H (2018) A facile in situ method to fabricate transparent, flexible polyvinyl alcohol/ZnO film for UV-shielding. *Compos Commun* 10:157–162. <https://doi.org/10.1016/j.coco.2018.09.009>
- [6] Li XX, Xu JK (2020) Synthesis of CdS QDs with single cubic and hexagonal lattice for blue-light-blocking nanocomposite films with a narrow absorbing transitional band. *Mater Today Commun* 24:101108. <https://doi.org/10.1016/j.mtcomm.2020.101108>
- [7] Li XX, Xu JK (2021) Blue-light-blocking CdS-PMMA nanocomposite films with tunable cut-off wavelength and narrow absorbing transitional band. *J Mater Sci-Mater El* 32:2113–2126. <https://doi.org/10.1007/s10854-020-04977-1>
- [8] Liu X, Zhou Q, Lin H, Wu J, Wu Z, Qu S, Bi Y (2019) The protective effects of blue light-blocking films with different shielding rates: a rat model study. *Transl Vis Sci Techn* 8:19–19. <https://doi.org/10.1167/tvst.8.3.19>
- [9] Beydaghyan G, Ajjou AN, Ashrit PV (2018) Fabrication of blue light-blocking optical interference coatings by the sol-gel method. *Appl Optics* 57:428–431. <https://doi.org/10.1364/AO.57.000428>
- [10] Huang GH, Huang YP, Xu W, Yao QH, Liu XF, Ding CF, Chen X (2019) Cesium lead halide perovskite nanocrystals for ultraviolet and blue light blocking. *Chinese Chem Lett* 30:1021–1023. <https://doi.org/10.1016/j.ccllet.2018.12.028>
- [11] Bisht A, Kumar V, Maity PC, Lahiri I, Lahiri D (2019) Strong and transparent PMMA sheet reinforced with amine functionalized BN nanoflakes for UV-shielding application. *Compos Part B-Eng* 176:107274. <https://doi.org/10.1016/j.compositesb.2019.107274>
- [12] Wang Y, Su J, Li T, Ma P, Bai H, Xie Y, Chen M, Dong W (2017) A novel UV-shielding and transparent polymer film: when bioinspired dopamine-melanin hollow nanoparticles join polymers. *ACS Appl Mater Inter* 9:36281–36289. <https://doi.org/10.1021/acsami.7b08763>
- [13] Adak B, Butola BS, Joshi M (2019) Calcination of UV shielding nanopowder and its effect on weather resistance property of polyurethane nanocomposite films. *J Mater Sci* 54:12698–12712. <https://doi.org/10.1007/s10853-019-0373-9>
- [14] Nguyen TV, Dao PH, Duong KL, Duongc QH, Vu QT, Nguyen AH, Mac VP, Le TL (2017) Effect of R-TiO<sub>2</sub> and ZnO nanoparticles on the UV-shielding efficiency of water-

- borne acrylic coating. *Prog Org Coat* 110:114–121. <https://doi.org/10.1016/j.porgcoat.2017.02.017>
- [15] Wang X, Zhou S, Wu L (2014) Fabrication of Fe<sup>3+</sup> doped Mg/Al layered double hydroxides and their application in UV light-shielding coatings. *J Mater Chem C* 2:5752–5758. <https://doi.org/10.1039/C4TC00437J>
- [16] Huang J, Chen H, Hao B, Dai W, Chen S (2019) Copolymerization strategy to prepare polymethyl methacrylate-based copolymer with broad-band ultraviolet shielding and luminescent down-shifting properties. *J Mater Sci* 54:14624–14633. <https://doi.org/10.1007/s10853-019-03961-3>
- [17] Man Y, Mu L, Wang Y, Lin S, Rempel GL, Pan Q (2015) Synthesis and characterization of rutile titanium dioxide/polyacrylate nanocomposites for applications in ultraviolet light-shielding materials. *Polym Composite* 36:8–16. <http://doi.org/10.1002/pc.22903>
- [18] Kikuchi A, Shibata K, Kumasaka R, Yagi M (2013) Excited states of menthyl anthranilate: a UV-A absorber. *Photochem Photobiol Sci* 12:246–253. <https://doi.org/10.1039/c2pp25190f>
- [19] Zhang Z, Chen K, Tang Q, Li H, Zou Z (2020) Hydrogen-bonding assembly of heteropolyacid and poly (vinyl alcohol) for strong, flexible, and transparent UV-protective films. *J Appl Polym Sci* 137:48813. <https://doi.org/10.1002/app.48813>
- [20] Singer S, Karrer S, Berneburg M (2019) Modern sun protection. *Curr Opin Pharmacol* 46:24–28. <https://doi.org/10.1016/j.coph.2018.12.006>
- [21] Li P, Wang S, Zhou SX (2020) Comfortable skin sunscreens based on waterborne cross-linkable polydimethylsiloxane coatings. *J Mater Chem C* 8:17383–17394. <https://doi.org/10.1039/d0tc04097e>
- [22] Yang Y, Ju Y, Li Y, Yin L, Chen L, Gu P, Zhang J (2020) Transparent nanostructured BiVO<sub>4</sub> double films with blue light shielding capabilities to prevent damage to ARPE-19 cells. *ACS Appl Mater Inter* 12:20797–20805. <https://doi.org/10.1021/acsami.9b22465>
- [23] Jiang YH, Shen HL, Huo XM, Li YF, Wang ML (2020) Effect of sputtering power on the structure and blue-light shielding capability of cuprous oxide thin films. *Opt Eng* 59:117101. <https://doi.org/10.1117/1.OE.59.11.117101>
- [24] Han C, Wang F, Gao C, Liu P, Ding Y, Zhang S, Yang M (2015) Transparent epoxy–ZnO/CdS nanocomposites with tunable UV and blue light-shielding capabilities. *J Mater Chem C* 3:5065–5072. <https://doi.org/10.1039/C4TC02880E>
- [25] Yang Y, Li Y, Yin L, Chen L, Zhang J (2019) Low cost ZnO/CdO thin films effectively reduce blue light-induced damage to RPE cells by display and lighting devices. *Mol Cryst Liq Cryst* 676:72–82. <https://doi.org/10.1080/15421406.2019.1596106>
- [26] Liu KQ, Kuang CX, Zhong MQ, Shi YQ, Chen F (2013) Synthesis, characterization and UV-shielding property of polystyrene-embedded CeO<sub>2</sub> nanoparticles. *Opt Mater* 35:2710–2715. <https://doi.org/10.1016/j.optmat.2013.08.012>
- [27] Zhao Y, Shi L, Tang A, Song N, Tang S, Ding P (2015) Enhanced blue light shielding property of light-diffusion polycarbonate composites by CeO<sub>2</sub>-coated silicate microspheres. *Funct Mater Lett* 8:1550074. <https://doi.org/10.1142/S1793604715500745>
- [28] Hsu CH, Liu TX, Hsieh IC, Han P, Lien SY (2016) Blue-light shielding, hard and hydrophobic inorganic and organic silicon stack-films prepared on flexible substrates. *Thin Solid Films* 618:146–150. <https://doi.org/10.1016/j.tsf.2016.03.055>
- [29] Pridmore RW (2021) Complementary colors: a literature review. *Color Res Appl* 46:482–488. <https://doi.org/10.1002/col.22576>
- [30] Yin XP, Zhang Z, Wu M, Zhang J, Xu GZ (2018) Toward transparent composite films with selective solar spectral, flame retardant and thermal insulation functions. *Mater Chem Phys* 216:365–371. <https://doi.org/10.1016/j.matchemphys.2018.06.028>
- [31] Herzog B, Wehrle M, Quass K (2009) Photostability of UV absorber systems in sunscreens. *Photochem Photobiol* 85:869–878. <https://doi.org/10.1111/j.1751-1097.2009.00544.x>
- [32] Paterson MJ, Robb MA, Blancafort L, DeBellis AD (2004) Theoretical study of benzotriazole UV photostability: ultrafast deactivation through coupled proton and electron transfer triggered by a charge-transfer state. *J Am Chem Soc* 126:2912–2922. <https://doi.org/10.1021/ja0386593>
- [33] Uesaka T, Ishitani T, Sawada R, Maeda T, Yagi S (2020) Fluorescent 2-phenyl-2H-benzotriazole dyes with intramolecular N-H...N hydrogen bonding: synthesis and modulation of fluorescence properties by proton-donating substituents. *Dyes Pigments* 183:108672. <https://doi.org/10.1016/j.dyepig.2020.108672>
- [34] Cui ZH, Li X, Wang XD, Pei KM, Chen WG (2013) Structure and properties of N-heterocycle-containing benzotriazoles as UV absorbers. *J Mol Struct* 1054:94–99. <https://doi.org/10.1016/j.molstruc.2013.09.045>
- [35] Kumasaka R, Kikuchi A, Yagi M (2014) Photoexcited states of UV absorbers, benzophenone derivatives. *Photochem Photobiol* 90:727–733. <https://doi.org/10.1111/php.12257>
- [36] Shi W, Zhang J, Shi XM, Jiang GD (2007) Influence of UV absorber on photodegradation processes of poly(vinyl chloride) with different average degrees of polymerization.

- Polym Eng Sci 47:1480–1490. <https://doi.org/10.1002/pen.20851>
- [37] Cong PL, Wang X, Xu PJ, Liu JF, He R, Chen SF (2013) Investigation on properties of polymer modified asphalt containing various antiaging agents. *Polym Degrad Stabil* 98:2627–2634. <https://doi.org/10.1016/j.polyimdegradstab.2013.09.024>
- [38] Oda H (2012) Improvement of light fastness of natural dye: effect of ultraviolet absorbers containing benzotriazolyl moiety on the photofading of red carthamin. *Color Technol* 128:108–113. <https://doi.org/10.1111/j.1478-4408.2011.00352.x>
- [39] Coltro L, Pitta JB, Madaleno E (2013) Performance evaluation of new plasticizers for stretch PVC films. *Polym Test* 32:272–278. <https://doi.org/10.1016/j.polymertesting.2012.11.009>

**Publisher's Note** Springer Nature remains neutral with regard to jurisdictional claims in published maps and institutional affiliations.